Synthesis, catalytic activity and phytotoxicity of a supported nickel(II) Schiff base complex

S. M. Islam · Sumantra Paul · Anupam Singha Roy ·
Satabdi Banerjee · Manir Mobarok ·
S. C. Santra

Abstract A supported Ni(II) complex has been synthesized and characterized by FTIR, UV–vis diffuse reflectance spectroscopy, thermogravimetric analysis and scanning electron microscopy. Its catalytic activity was evaluated for alkyne–azide coupling and benzothiazole synthesis. These reactions were found to require mild conditions, reaction times, and most importantly, could be carried out in aqueous medium. The catalyst could be easily recovered and reused five times without significant decrease in its activity. Leaching tests indicated that the catalyst is truly heterogeneous. The nickel complex was tested for its inhibition of germination of MTU 7029 seeds. Rice (MTU 7029, *Oryza sativa*) is a staple crop in southeast Asia.

Introduction

Dipolar cycloadditions have captured the attention of organic chemists since their discovery over 50 years ago by Robert Huisgen [1, 2]. In 2002, the Huisgen 1,3-dipolar cycloaddition of terminal alkynes and organic azides catalyzed by homogeneous Cu(I) salts was accomplished

S. M. Islam (✉) · S. Paul · A. S. Roy · M. Mobarok
Department of Chemistry, University of Kalyani, Kalyani,
Nadia 741235, W.B., India
e-mail: manir65@rediffmail.com

S. Banerjee · S. C. Santra
Department of Environment Science, University of Kalyani,
Kalyani, Nadia 741235, W.B., India

independently by both Sharpless and Meldal [3, 4]. The rich yet elusive mechanistic variability of this reaction has engendered a large number of procedures developed for specific substrate classes and environmental constraints [5]. Although the reaction is highly exothermic, cycloadditions involving inactivated substrates are often very slow, even at elevated temperatures (80–120 °C for 12–24 h), due to the high activation barrier (ca. 25–26 kcal/mol for reaction of methyl azide with propyne) [6, 7]. More recently, catalysts have been developed for these reactions, producing the 1,4-regioisomers exclusively under mild conditions. These reactions are also an example of click chemistry [8, 9]. Their 100 % atom economy and simple purification have led to various applications for agrochemicals, material science, biochemistry and functional materials. Triazoles containing three nitrogen atoms in the five-membered aromatic azole ring are readily able to bind with a variety of enzymes and receptors in biological systems via non-covalent interactions, and thus display versatile biological activities. Although the 1,2,3-triazole structural moiety does not occur in nature, it may display biological activity, and there are numerous examples in the literature including anti-HIV activity, anticancer agents, anti-mycobacterium agents, antimicrobial activity against Gram-positive bacteria, anti-allergies, anticonvulsants, β-lactamase inhibitors and selective β3 adrenergic receptor agonists. [10–16].

2-Aryl benzothiazoles are important molecules due to their use not only as medicinal agents but also as organic functional materials such as fluorescent dyes and liquid crystals [17–19]. These structural motifs often possess interesting biological and physical properties and have been extensively applied in the preparation of pharmaceuticals, advanced materials and solar cells [20–24]. Although the preparation of such molecules is typically

catalyzed by Pd, Rh, Ir and Ru complexes, catalytic systems using inexpensive metals such as Cu, Ni and Fe are also emerging [25–27].

Immobilization of metal complexes onto solid supports is highly desirable for the development of reusable catalysts [28, 29]. Surface functionalization and incorporation of metal complexes is one of the general methods for preparation of supported catalysts. Many solid supports including graphene, nanostructured silica [30, 31], hierarchical zeolites [32] and 3D ordered mesoporous materials [33] are being studied exclusively at present. Also polymers such as chloromethyl polystyrene, syndiotactic polystyrene and

other functionalized polystyrenes are of interest in the field of supported catalysts because of their low cost and easy separation from the reaction mixture [34–36].

Motivated by the fact that arylated azoles are privileged structures present in many biologically active molecules, we have been exploring the synthesis of azoles using heterogeneous Ni(II) catalysts. The present work describes a one-pot synthesis of 1,2,3-triazole and benzothiazole derivatives under mild conditions, using a supported Ni(II) catalyst. The free complex is also an effective inhibitor of MTU 7029 (*Oryza sativa*) seed germination.

Experimental

Materials and measurements

All the reagents used were of analytical reagent grade. The solvents were dried and distilled before use by following the standard procedures [37]. Merrifield resin was purchased from Sigma-Aldrich. Other reagents were obtained from Merck or Fluka.

A Perkin-Elmer 2400 C elemental analyzer was used to collect microanalytical data (C, H and N). Nickel content

Table 1 Chemical composition of solid Ni(II) complex

Compound	C (%)	H (%)	N (%)	Cl (%)	Metal (%)
Merrifield resin	70.9 (70.8)	6.0 (5.9)	–	23.3 (23.2)	–
PS-L	76.6 (76.5)	6.0 (5.9)	11.2 (11.1)	3.39	–
PS-Ni(ii)-L	68.8 (68.7)	5.1 (5.0)	10.1 (10.0)	3.35	3.1

Calculated values are given in parentheses
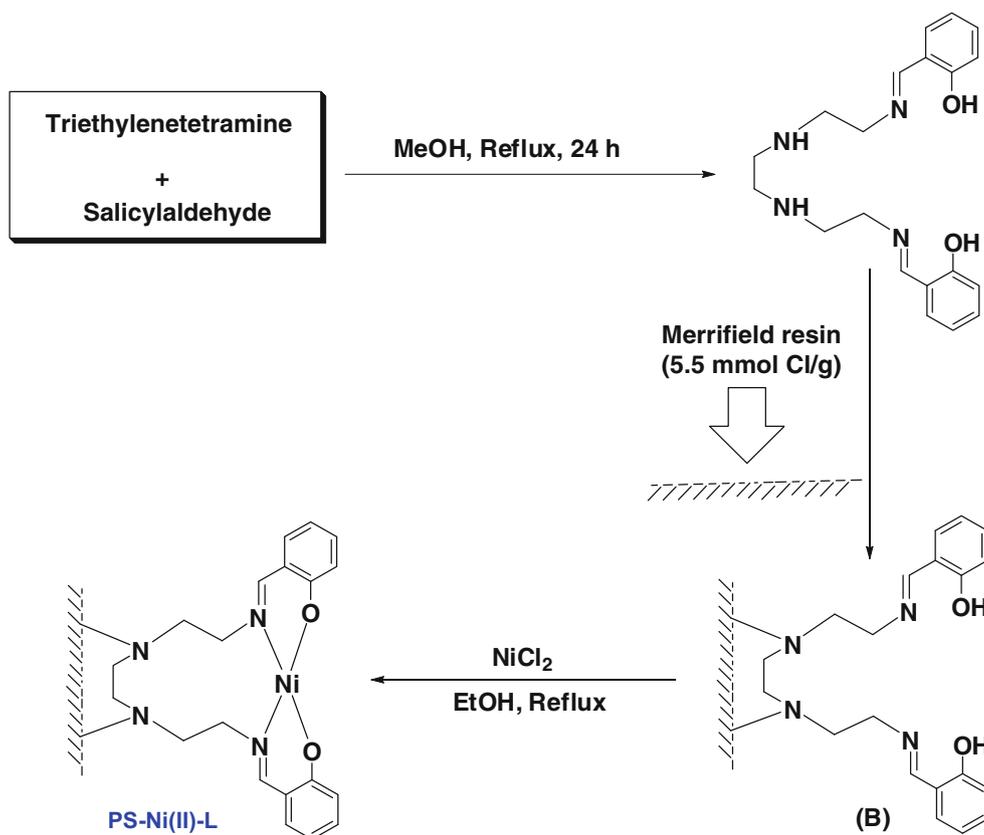
Scheme 1 Synthesis of the polymer-supported metal complex

of the sample was measured with a Varian AA240 atomic absorption spectrophotometer (AAS). FTIR spectra were recorded on a Perkin-Elmer FT-IR 783 spectrophotometer using KBr pellets. Diffuse reflectance spectra (DRS) were recorded on a Shimadzu UV/3101 PC spectrophotometer. A Mettler Toledo TGA/SDTA 851 instrument was used for thermogravimetric analysis (TGA). Morphologies of the functionalized polystyrene and immobilized complex were analyzed using a scanning electron microscope (SEM, ZEISS EVO40, England) equipped with EDX facility.

Synthesis of the Schiff base (L)

Triethylenetetramine was mixed with salicylaldehyde (1:2 molar ratio) in methanol (10 mL) at 60 °C with stirring for 24 h. The mixture was then cooled to room temperature and filtered. The yellow residue was washed with ethanol until the filtrate became colorless and dried under vacuum (∼79 % yield).
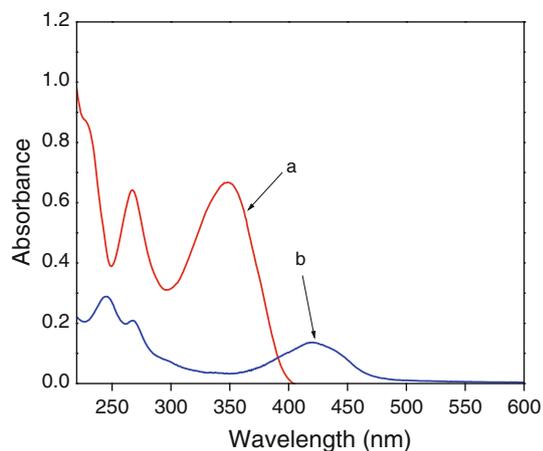
Fig. 1 DRS–UV–visible absorption spectra of solid Schiff base ligand (*a*) and solid complex, PS-Ni(II)-cat (*b*)

Synthesis of polymer-anchored ligand, PS-L

A solution of the Schiff base ligand L (2.8 mmol) in methanol (20 mL) was added to 1.0 g of Merrifield resin (5.5 mmol Cl/g loading), and the mixture was heated to reflux with continuous stirring for 24 h. After refluxing, the mixture was cooled to room temperature and then filtered. The yellow beads were washed with cold 1:1 methanol–water mixture until the filtrate became colorless and finally dried under vacuum to give PS-L (1.0 g).
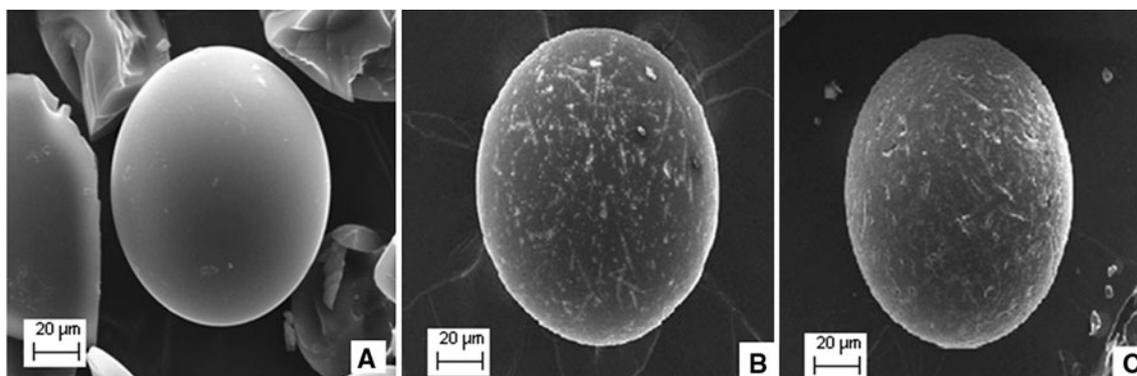
Synthesis of the supported complex

A solution of $NiCl_2$ in ethanol (20 mL, 1 % wt/v) was added dropwise to 1.0 g of PS-L over a period of ca. 45 min under constant stirring. Then, the reaction mixture was refluxed for 24 h. The product was filtered off, washed thoroughly with ethanol and dried at room temperature under vacuum to give PS-Ni(II)-L (1.0 g).
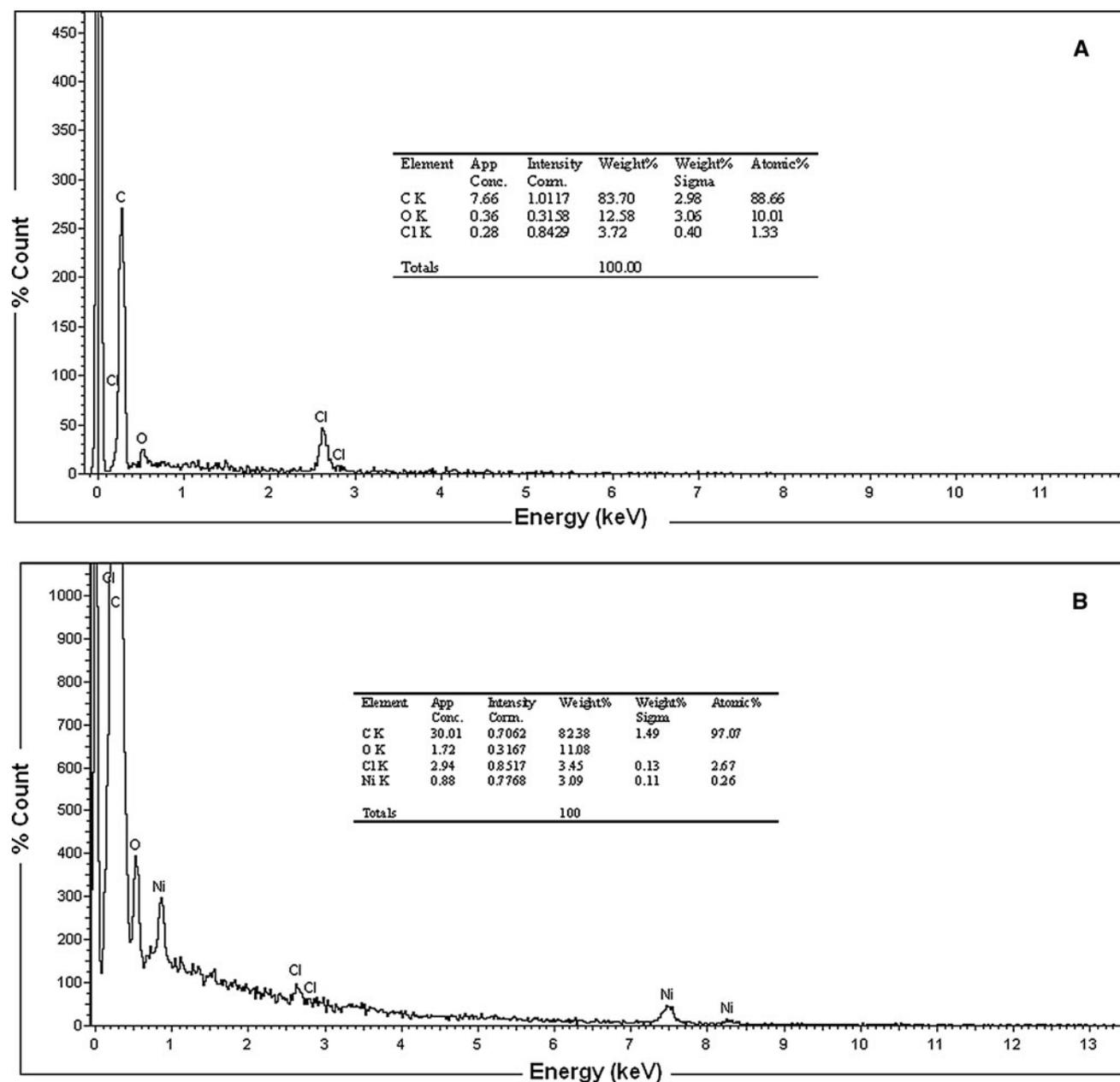
Synthesis of the free complex

The Schiff base ligand (1.53 g, 5 mmol) was mixed with a solution of $NiCl_2$ (1.18 g, 5 mmol) under constant stirring. Then, the reaction mixture was refluxed for 6 h. After completion of the reaction, the mixture was cooled, whereupon the Ni(II) complex was precipitated out. It was collected and carefully washed with ice-cold ethanol (Yield 1.05 g, 58 %).

General procedure for 1,2,3-triazole synthesis

In a 50-mL round-bottom flask, the required benzyl halide (1.0 mmol), sodium azide (0.065 g), aryl alkyne (1.0 mmol) and PS-Ni(II)-L (50 mg) were stirred in distilled water (10 mL). The reaction was allowed to proceed for 6 h at room temperature under argon atmosphere. After completion of the reaction, the organic products were extracted out with ethyl acetate (5 mL × 2). The combined organic layer

Fig. 2 FE-SEM images of polymer-anchored ligand (**a**) and polymer-anchored Ni(II) complex (**b**)

Element	App Conc.	Intensity Corn.	Weight%	Weight% Sigma	Atomic%
C K	7.66	1.0117	83.70	2.98	88.66
O K	0.36	0.3158	12.58	3.06	10.01
Cl K	0.28	0.8429	3.72	0.40	1.33
Totals			100.00		

Element	App Conc.	Intensity Corn.	Weight%	Weight% Sigma	Atomic%
C K	30.01	0.7062	82.38	1.49	97.07
O K	1.72	0.3167	11.08		
Cl K	2.94	0.8517	3.45	0.13	2.67
Ni K	0.88	0.7768	3.09	0.11	0.26
Totals			100		

Fig. 3 EDX images of polymer-anchored ligand (a) and polymer-anchored Ni(II) complex (b)

was dried over Na_2SO_4, and the solvent was removed under reduced pressure. Reactions were monitored by TLC using aluminum-backed silica gel 60 (F254) plates, visualized using UV254 nm, and potassium permanganate and ninhydrin dips as appropriate, and purified by silica gel column chromatography. All reaction products were identified by NMR spectroscopy.

General procedure for benzothiazole synthesis

2-mercapto aniline or it derivatives (1.0 mmol), aromatic aldehyde (1.0 mmol), water (10 mL) and PS-Ni(II)-L

(50 mg) were charged into a 50-mL round-bottom flask. The reaction mixture was stirred at 50 °C for 12 h under argon atmosphere, then cooled to room temperature and extracted with ethyl acetate (5 mL × 2). The organic layer was dried over Na_2SO_4, and the solvent was removed under reduced pressure. Reactions were monitored by TLC using aluminum-backed silica gel 60 (F254) plates, visualized using UV254 nm, potassium permanganate and ninhydrin dips as appropriate and purified by silica gel column chromatography. All reaction products were identified by NMR spectroscopy.
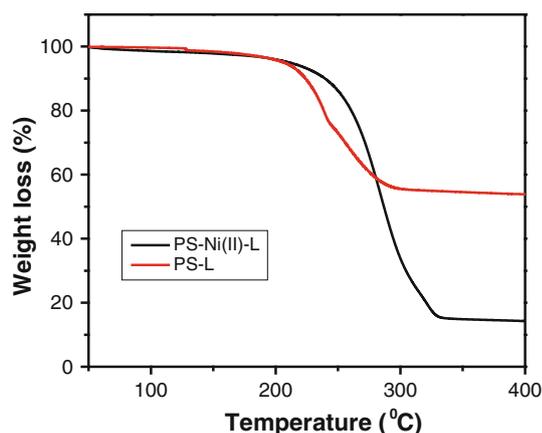
Fig. 4 Thermogravimetric weight loss plots for solid Ni(II) complex

Fig. 5 Optimization of temperature during alkyne–azide coupling catalyzed by solid Ni(II) complex. Reaction condition: [benzyl chloride] = 1 mmol, [phenylacetylene] = 1 mmol, NaN$_3$ (0.065 g), water (10 mL), room temperature

Table 2 Optimization of solvent during alkyne–azide coupling catalyzed by solid Ni(II) complex

Entry	Solvent	Conversion (%)	[Yield (%)][a]	Selectivity (%) (in approx)
1	Toluene	39	18	46
2	THF	30	16	53
3	Acetone	45	27	60
4	DCM	43	27	63
5	MeCN	49	30	61
6	EtOH	52	33	63
7	DMSO	56	37	66
8	Ethanol–water mix(1:1)	60	39	65
9	DMSO–water mix(1:1)	65	46	71
10	Water	96	90	94
11[b]	Water	78	72	92
12[c]	Water	98	93	95

Reaction condition: [benzyl chloride] = 1 mmol, [phenylacetylene] = 1 mmol, NaN$_3$ (0.065 g), Solvent (10 mL) room temperature, catalyst 50 mg (2.6×10^{-2} mmol). Reaction time 6 h

Products are characterized by NMR spectroscopy

[a] Isolated yields after silica gel column chromatography
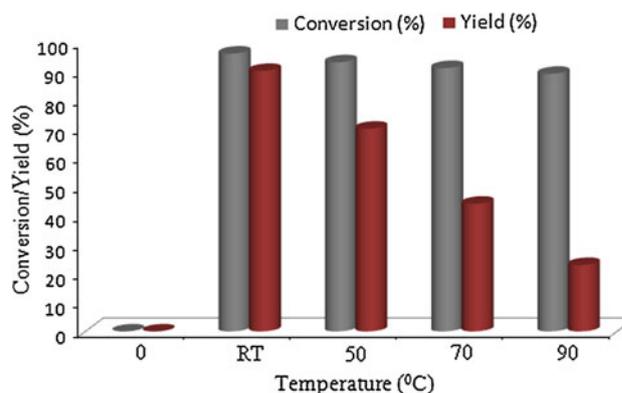
[b] [phenylacetylene] = 0.5 mmol

[c] [phenylacetylene] = 1.5 mmol,

Selectivity $(\%) = \dfrac{\text{Product formed (moles)}}{\text{Substrate Converted (moles)}} \times 100$

Fig. 6 Optimization of temperature during benzothiazole synthesis catalyzed by solid Ni(II) complex. Reaction condition: [2-mercapto aniline] = 1 mmol, [aldehyde] = 1 mmol, water (10 mL), at 50 °C, catalyst 50 mg
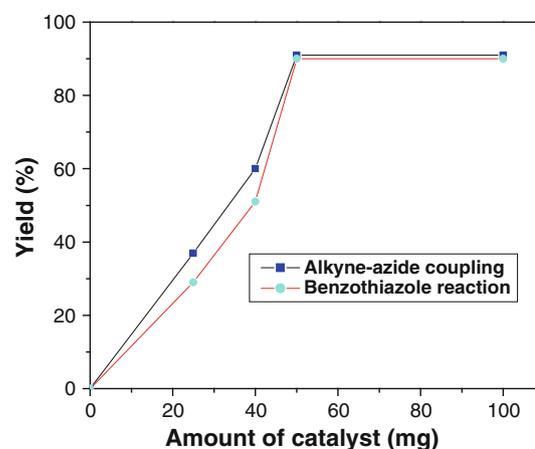
Results and discussion

Characterization of the supported complex

The Schiff base ligand obtained from the reaction of salicylaldehyde with triethylenetetramine has been well characterized as described previously [38]. Due to the insolubility of the polymer-supported metal complex in all common solvents, its structural investigation was limited to physicochemical properties, chemical analysis, SEM, TGA, FT-IR and UV–vis spectral data. Table 1 provides the analytical data, which show a 1:1 ratio of metal to Schiff base ligand. The metal content of the solid catalyst was estimated by atomic absorption spectrometry. The chemical composition confirmed the purity and stoichiometry of the neat and supported complexes (Scheme 1).

IR and UV spectroscopy

Attachment of the metal to the support was confirmed by comparison of the FTIR spectra (Fig. S1) of the polymers before and after loading with nickel, both in the mid-IR (4,000–400 cm^{-1}) and far-IR (600–50 cm^{-1}) regions. The

Table 3 Alkyne-azide coupling catalyzed by solid Ni(II) complex
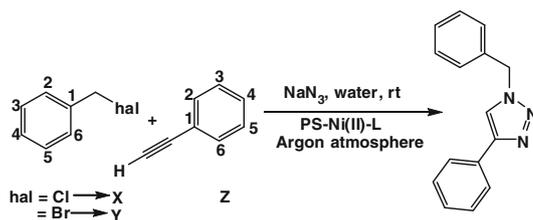
| Sl. No.	Ar-CH₂-X	Aryl alkyne	Product[a]	Yield (%)/ Selectivity (%)[b]
1	**X**	**Z**		90/94
2	4-OH-**X**	**Z**		93/95
3	4-(OCH₃)-**X**	**Z**		91/95
4	4-(NO₂)-**X**	**Z**		82/90
5		**Z**		86/91
6	Y	n-Hexyl———H		73/85
7	Y			84/90
8	Y	(4-OCH₃)-**Z**		92/93
9	Y	4-Me-**Z**		89/92
10	4-(OCH₃)-**X**			82/89

Reaction condition: [benzyl halide] = 1 mmol, [alkyne] = 1 mmol, NaN₃ (0.065 g), water (10 mL), room temperature, catalyst 50 mg (2.6×10^{-2} mmol). Reaction time 6 h

[a] Products are characterized by NMR spectroscopy

[b] Isolated yields after silica gel column chromatography

IR spectrum of pure Merrifield resin has an absorption band at 1,261 cm^{-1} due to the C–Cl group, which was absent from the spectra of the resin-bound ligand and catalyst. A stretching vibration assigned to CH$_2$ is observed at 2,918 cm^{-1} for the polymer-bound ligand and its complex. The stretching vibrations of the C=N bonds appeared at around 1,630–1,655 cm^{-1} for the free and supported Schiff base; the bond is lowered to 1,590–1,615 cm^{-1} in the nickel complex, indicating the coordination of azomethine nitrogen to the metal [39]. A peak at 3,433 cm^{-1} for the secondary amine (–NH–) group of the free Schiff base is absent in the polymer-bound Schiff base ligand. Another band at 3,325 cm^{-1} is noticed for O–H stretching, which is not observed for the metal complex, as the –OH group coordinates to nickel through the deprotonated oxygen. Peaks assigned to Ni–O for the metal complexes are observed around 645–630 cm^{-1} [39]. In the far-IR spectra, bands due to the Ni–N stretching vibration are observed around 520–580 cm^{-1} [40]. In the free Schiff base ligand, the C–O bond appears at 1,270 cm^{-1} and it is changed to 1,320 cm^{-1} for PS-Ni(II)-L, confirming the metal oxygen coordination [41, 42].

The electronic spectrum of the polymer-supported metal complex was recorded in diffuse reflectance spectrum (DRS) mode as MgCO$_3$/BaSO$_4$ disks, due to the solubility limitations. The UV–vis spectrum of the polymer-anchored complex PS-Ni(II)-L is given in Fig. 1. The reflectance spectrum of the PS-L shows bands at 265 and 348 nm assigned to n–π* and π–π* transitions. PS-Ni(II)-L exhibits three bands at 245, 268 and 421 nm; the first two are due to charge transfer, and the last one may be assigned to a d–d transition [43].
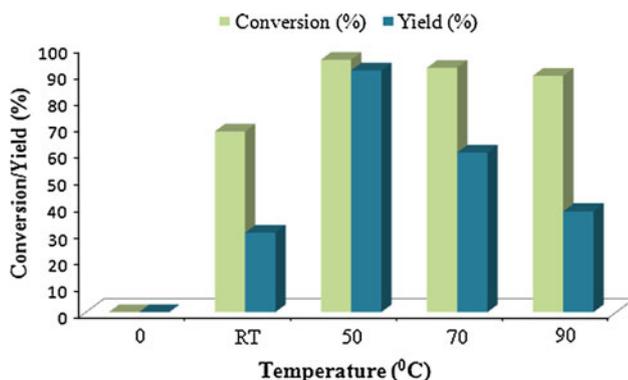
Fig. 7 Optimization in amount of catalyst during alkyne–azide coupling and benzothiazole synthesis catalyzed by solid Ni(II) complex. Reaction condition: [benzyl chloride] = 1 mmol, [phenylacetylene] = 1 mmol, NaN$_3$ (0.065 g), water (10 mL), room temperature and [2-mercapto aniline] = 1 mmol, [aldehyde] = 1 mmol, water (10 mL), at 50 °C, catalyst 50 mg

SEM and EDAX analysis

Field emission-scanning electron micrographs of single beads of pure chloromethylated polystyrene, polymer-anchored ligand (PS-L) and its complex PS-Ni(II)-L revealed that morphological changes occurred on the polystyrene beads at various stages of the synthesis. The SEM images of polymer-anchored ligand (A) and the immobilized Ni(II) complex (B) on functionalized polymer are shown in Fig. 2. The pure chloromethylated polystyrene beads have a smooth surface (not shown) while the polymer-anchored ligand and complex show slight roughening of the top layer of the beads. Energy-dispersive X-ray analyses (EDX) of the immobilized complex showed the metal content along with C, N, O and Cl, suggesting formation of the metal complex with the anchored ligand at various sites (Fig. 3). The ratios of metals to other elements obtained from EDX analysis are quite similar to the data obtained from elemental analysis.

TGA studies

The thermal stability of complex was investigated using TGA at a heating rate of 10 °C/min in air over a temperature range of 30–600 °C. TGA curves of the polymer-anchored ligand and nickel complex are shown in Fig. 4. The polymer-anchored ligand decomposed in the temperature range 190–200 °C (data not shown). The polymer-supported Ni(II) Schiff base complex decomposed at 240 °C. Hence, it can be concluded that the polymer-supported metal complex degrades only at high temperature.

Catalytic synthesis of 1,2,3-triazoles

To test the catalytic activity of the present catalyst, the coupling of phenyl acetylene and benzyl chloride was chosen as a probe reaction. We took sodium azide as the only azide source for this reaction. In order to optimize the conditions for use of PS-Ni(II)-L, we have studied this reaction in various polar and non-polar solvents. Water proved to be a suitable solvent, giving the best results for alkyne–azide coupling reactions in the presence of the supported catalyst (Table 2). Furthermore, increasing the water content in the solvent medium increases the yield (Table 2, Entries 8–10). The reactions were also studied in different temperature ranges (from 0 to 90 °C), and the present catalytic system gave good results at room temperature under argon atmosphere (Fig. 5). We found that 50 mg of catalyst was sufficient to produce high yields; use of greater amounts of catalyst did not improve the yield (Fig. 6). All the substituted 1,2,3-triazoles were therefore synthesized under these optimized conditions. The results are summarized in Table 3 and show that these reactions

Table 4 Synthesis of benzothiazole using solid Ni(II) complex
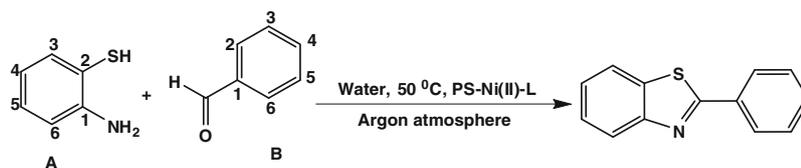
Sl. No.	Mercaptoanilines	Aromatic aldehyde	Product[a]	Yield (%)/ Selectivity (%)[b]
1	A	B		91/95
2	A	4-Cl-B		93/95
3	A	4-Br-B		85/92
4	A	4-Me-B		80/86
5	A	2-OH-B		90/94
6	A	2-Cl-B		84/90
7	A	3-(OCH$_3$)-B		82/91
8	A	3,4-(OCH$_3$)-B		91/93
9	A	Napthal-2-yl		79/87
10	5-Cl-A	B		73/85

Reaction condition: [mercapto aniline] = 1 mmol, [aldehyde] = 1 mmol, water (10 mL), at 50 °C, catalyst 50 mg (2.6 × 10^{-2} mmol). Reaction time 12 h

[a] Products are characterized by NMR spectroscopy

[b] Isolated yields after silica gel column chromatography

Table 5 Recycling efficiency of PS-Ni(II)-L complex in alkyne–azide coupling and benzothiazole synthesis

Reactions	Run 1	Run 2	Run 3	Run 4	Run 5
Alkyne–azide coupling	90	90	88	87	86
Benzothiazole synthesis	91	90	90	88	87

are highly selective. Substrates were selected varying both the aromatic halides (Entry 1–5) and the alkynes (Entry 6–10). It is noticeable that electron-donating substituents

on the benzyl moiety increase the yield, whereas it decreases with substrates containing electron deficient aromatic halides. The same observation was found for the different alkynes studied.

Catalytic synthesis of benzothiazole

In continuation of our interest in azole synthesis, we decided to synthesize another important class of azoles, namely benzothiazoles. These are usually synthesized mainly by three-phase coupling among aromatic amines,

Table 6 Phytotoxicity assay over MTU 7029 catalyzed by neat Ni(II) Schiff base complex

Sl. No.	Parameter	Control	Treatment with nickel salt/complex					
			Nickel nitrate [Ni(NO$_3$)$_2$]			Ni(II) Schiff base complex		
			300 ppm	350 ppm	400 ppm	300 ppm	350 ppm	400 ppm
1	Catalase (µg/g tissue)	22.4 ± 1.25	21.5 ± 1.7	22.1 ± 0.5	22.3 ± 0.7	22.4 ± 0.9	22.2 ± 1	21.8 ± 2.1
2	Amylase (mg/g tissue)	39 ± 2.1	78 ± 3.2	80 ± 4.6	92 ± 4.2	110 ± 9.3	112 ± 6.3	118 ± 4
3	Ascorbic acid (mg/100 g sample)	600 ± 10	560 ± 7	200 ± 8	120 ± 7	480 ± 9	400 ± 4.5	280 ± 9
4	Carbohydrate (mg/g in 100 g sample)	680 ± 5	480 ± 6	340 ± 6	236 ± 12	380 ± 6	308 ± 11	180 ± 4
5	Protein (µmol/g tissue)	0.20 ± 0.02	0.03 ± 0.009	0.06 ± 0.01	0.07 ± 0.01	0.11 ± 0.009	0.18 ± 0.02	0.23 ± 0.03
6	Germination (%)	100	80	75	60	60	60	30

aldehydes and sulfur agent like CS$_2$, sulfur powder and K$_2$SO$_8$. As sulfur-donating agents are toxic and may cause unwanted interference with the products, in order to minimize their use in the reaction medium, we chose an alternative method in which 2-mercaptoanilines are coupled with aromatic aldehydes in appropriate ratio. For simplicity, coupling between 2-mercaptoaniline and benzaldehyde was chosen as the primary reaction in order to study the catalytic activity of PS-Ni(II)-L. The reaction conditions were optimized in water as solvent. The effect of temperature was also studied, and 50 °C was taken as the optimum temperature (Fig. 7). At room temperature, the yield is low; hence, heating is needed to activate this type of coupling. All the reactions were carried out with 50 mg of catalyst (Fig. 6). Under the optimized conditions, PS-Ni(II)-L give good yields of all the substituted benzothiazoles, with high selectivities also. Benzaldehydes containing electron-donating and electron-withdrawing groups were employed to afford the corresponding benzothiazoles in yields ranging from 77 to 93 %; no significant substituent effects were observed. The results are shown in Table 4.

Stability and recycling of the catalyst

The leaching of metal from the supported nickel(II) complex was investigated by carrying out analysis of the used catalyst (EDX, IR) as well as the product mixtures (AAS, UV–vis). Analysis of the used catalyst did not show any appreciable loss in the nickel content compared to the fresh catalyst. The IR spectrum of the recycled catalyst was similar to that of fresh sample. Analysis of the product mixtures showed no detectable nickel content. The UV–vis spectra of the reaction solution obtained after the first run did not show any absorption peaks characteristic of nickel metal, again indicating that the leaching of metal did not take place during the course of the reaction. The metal content of the recycled catalyst was determined with the help by AAS and found to be virtually unaltered. These observations confirm that the present catalyst is truly heterogeneous in nature.

A heterogeneity test was also carried out for benzothiazole synthesis as an example. The catalyst was filtered out from the reaction mixture at 50 °C after 4 h, and the filtrate was allowed to react up to the completion of the reaction (6 h). The reaction mixture from 4 h and the filtrate were then analyzed by gas chromatography. No changes in the conversion or selectivity were found, confirming that the catalyst was heterogeneous in nature.

Next, the used catalyst was recovered, washed with water, dichloromethane and acetone, and dried at 100 °C. A reaction between benzyl chloride and phenylacetylene was then carried out with the recycled catalyst under the optimized reaction conditions. Similarly, the recycled catalyst was tested for benzothiazole synthesis from 2-mercaptoaniline and benzaldehyde under the optimized conditions. The results are given in Table 5. As seen from Table 5, the recycled catalyst did not show any appreciable loss in activity, which indicates that the catalyst is stable under the reactions condition and can be used for up to five consecutive runs.

Phytotoxicity assay

The methodology for the phytotoxicity assay is given in the supplementary section. Phytotoxicity can be determined in a number of ways, one of which is a seed germination test [44]. Metals can strongly influence seed germination [45]. In general, nickel has relatively low toxicity [46].

For the present complex, the extent of germination varied with the dose. No germination was observed at 500 ppm, whereas 100 % germination was observed for the control set. The simple salt nickel nitrate also decreased the extent of germination.

Five parameters were analyzed for seed germination at concentrations of 300, 350 and 400 ppm, and the results are summarized in Table 6. No significant change in catalase activity was observed. Both carbohydrate and ascorbic acid content decreased with increased dose, and contents were higher for nickel nitrate than for the nickel(II) complex. Amylase and proline content both increased with increasing dose, and the contents were higher for the nickel complex than for nickel nitrate.

Conclusions

A supported nickel(II) complex was prepared and characterized. This complex proved to be an active catalyst for the one-pot synthesis of various substituted azoles in water medium. The catalyst is cheap, air stable and recyclable under the reaction conditions used. The homogeneous complex is bioactive and inhibits the germination of MTU 7029. We hope that this complex will find importance in industrial applications.

References

1. Huisgen R (1961) Proc Chem Soc London 1961:357–369
2. Huisgen R (1963) Angew Chem Int Ed Engl 1963:565–598
3. Rostovtsev VV, Green LG, Fokin VV, Sharpless KB (2002) Angew Chem 114:2708–2711
4. Tornoe CW, Christensen C, Meldal M (2002) J Org Chem 67:3057–3064
5. Meldal M, Tornoe CW (2008) Chem Rev 108:2952–3015
6. Jewett JC, Bertozzi CR (2010) Chem Soc Rev 39:1272–1279
7. Himo F, Lovell T, Hilgraf R, Rostovtsev VV, Noodleman L, Sharpless KB, Fokin VV (2005) J Am Chem Soc 127:210–216
8. Thirumurugan P, Matosiuk D, Jozwiak K (2013) Chem Rev 113:4905–4979
9. Iha RK, Wooley KL, Nyström AM, Burke DJ, Kade MJ, Hawker CJ (2009) Chem Rev 109:5620–5686
10. Qian K, Bori ID, Chen CH, Huang L, Lee KH (2012) J Med Chem 55:8128–8136
11. Li WT, Wu WH, Tang CH, Tai R, Chen ST (2011) ACS Comb Sci 13:72–78
12. Service RF (2008) Science 322:868–869
13. Isobe H, Fujino T, Yamazaki N, Nieckowski MG, Nakamura E (2008) Org Lett 10:3729–3732
14. Lubell WD (2012) Org Lett 14:4297–4302
15. Ko E, Liu J, Perez LM, Lu G, Schaefer A, Burgess K (2011) J Am Chem Soc 133:462–477
16. Kharb R, Sharma PC, Yar MS (2011) J Enzyme Inhib Med Chem 26:1–21
17. Siddiqui N, Rana A, Khan SA, Bhat MA, Haque SE (2007) Bioorg Med Chem Lett 17:4178–4182
18. Schwander H (1988) In: Hendrix P (ed) Ullman's encyclopedia of industrial chemistry. VCH, Weinheim, p 279
19. Mori A, Sekiguchi A, Masui K, Shimada T, Horie M, Osakada K, Kawamoto M, Ikeda T (2003) J Am Chem Soc 125:1700–1701
20. McNally A, Prier CK, MacMillan DWC (2011) Science 334:1114–1117
21. Muto K, Yamaguchi J, Itami K (2012) J Am Chem Soc 134:169–172
22. Wang L, He W, Yu Z (2013) Chem Soc Rev 42:413–420
23. Naumov P, Kochunnoony M (2010) J Am Chem Soc 132:11566–11579
24. Zhu W, Wu Y, Wang ZS, Li W, Li X, Chen J, Wang Z, Tian H (2011) Adv Funct Mater 21:756–763
25. Lipshutz BH, Nihan DM, Vinogradova E, Taft BR, Bošković ŽV (2008) Org Lett 10:4278–4279
26. González J, Pérez VM, Jiménez DO, Lopez-Valdez G, Corona D, Cuevas-Yañez E (2011) Tetrahedron Lett 52:3514–3517
27. Hudson R, Li CJ, Moores A (2012) Green Chem 14:622–624
28. Pittman CU Jr, Carraher CE Jr (2007) Chapter 1, Organometallic polymers: the early days. In: Aziz AE, Manners I (eds) Frontiers in transition metal-containing polymers. Wiley Interscience, Weinheim
29. Parihar S, Pathan S, Jadeja RN, Patel A, Gupta VK (2012) Inorg Chem 51:1152–1161
30. Campos JM, Lourenço JP, Cramail H, Ribeiro MR (2012) Prog Polym Sci 37:1764–1804
31. Kuilla T, Bhadra S, Yao D, Kim NH, Bose S, Lee JH (2010) Prog Polym Sci 35:1350–1375
32. Ishihara A, Inui K, Hashimoto T, Nasu H (2012) J Catal 295:81–90
33. Liu Y, Dai H, Du Y, Deng J, Zhang L, Zhao Z, Au CT (2012) J Catal 287:149–160
34. Maurya MR, Kumar A, Pessoa JC (2011) Coord Chem Rev 255:2315–2344
35. Aziz ASAE, Harvey P (ed) (2004) In: Organometallic and coordination clusters and polymers: syntheses and applications, Macromolecular Symposia. Wiley, Weinheim
36. Schellenberg J (2009) Prog Polym Sci 34:688–718
37. Vogel AI (1989) Test book of practical organic chemistry, 5th edn. Longman, London
38. Paital AR, Wong WT, Aromí G, Ray D (2007) Inorg Chem 46:5727–5733
39. Khandar AA, Cardin C, Hosseini-Yazdi SA, McGrady J, Abedi M, Zarei SA, Gan Y (2010) Inorg Chim Acta 363:4080–4087
40. Sallam SA, Orabi AS (2002) Transit Met Chem 27:447–453
41. Patel BV, Desai K, Thaker T (1989) Synth React Inorg Met Org Chem 19:391
42. Marvel CS, Aspey SA, Dudley EA (1956) J Am Chem Soc 78:4905–4909
43. Sacconi L (1968) Transit Met Chem 61:943
44. Iersel MWV, Bugbee B (1996) J Am Soc Hortic Sci 121:1095–1102
45. Kranner I, Colville L (2011) Environ Exp Bot 72:93–105
46. Weng L, Lexmond TM, Wolthoorn A, Temminghoff EJM, Riemsdijk WHV (2003) Environ Toxicol Chem 22:2180–2187